LJMU Research Online

Messina, M and Njuguna, J

 Potential of silicon nanowires structures as nanoscale piezoresistors in mechanical sensors

http://researchonline.ljmu.ac.uk/id/eprint/1964/

Article

For more information please contact researchonline@ljmu.ac.uk

Potential of silicon nanowires structures as nanoscale piezoresistors in mechanical sensors

Potential of silicon nanowires structures as nanoscale piezoresistors in mechanical sensors

M Messina and J Njuguna

Cranfield University, Cranfield Campus, Bedfordshire, UK

E-mail:j.njuguna@cranfield.ac.uk

Abstract. This paper presents the design of a single square millimeter 3-axial accelerometer for bio-mechanics measurements that exploit the potential of silicon nanowires structures as nanoscale piezoresistors. The main requirements of this application are miniaturization and high measurement accuracy. Nanowires as nanoscale piezoresistive devices have been chosen as sensing element, due to their high sensitivity and miniaturization achievable. By exploiting the electro-mechanical features of nanowires as nanoscale piezoresistors, the nominal sensor sensitivity is overall boosted by more than 30 times. This approach allows significant higher accuracy and resolution with smaller sensing element in comparison with conventional devices without the need of signal amplification.

1. Introduction

Silicon nanowires have a very large piezoresistance effect [1-5], capable of enhancing the mechanical sensors performance, which is now actively being explored to improve silicon transistors [6], [7]. Silicon nanowires are also attractive for applications in the filed-emission devices, photonics, chemical sensors and spintronics [8]. The piezoresistive effect is used for transducing, for example, acceleration in an electrical output. After an inertial force is applied to the sensor the strain on the piezoresistive material (silicon) changes its electrical resistance proportionally, therefore the correspondent voltage change is a measure of the acceleration by less than a constant of proportionality.

In the last decade experimental studies on the piezoresistance effect of SiNWs agreed that SiNWs under uniaxial stress offer an enhanced piezoresistance effect with respect to the bulk counterparts [1-5], [9], [10], [11]. The origin and behavior of this phenomenon called in the literature "Giant Piezoresistance", is currently not clearly understood and research is at infancy stage. This effect would be of enormous impact on the performance of mechanical sensor. To date, relatively few reports on the development of silicon nanowire-based sensors are available [12], [13]. However, p-type single crystalline SiNWs have been studied for sensor applications [4], [9], [10], [14], [16].

Toriyama et al. [9] studied silicon nanowire piezoresistors fabricated by separation of implanted oxygen (SIMOX), thermal diffusion, electron beam (EB) direct writing, and reactive ion etching (RIE). In their study longitudinal and transverse piezoresistive coefficients, $\pi_{l\ <110>}$ and $\pi_{t\ <110>}$, were both dependant on the cross sectional area of the nanowires. The $\pi_{l\ <110>}$ of the nanowire piezoresistors increased (up to 60%) with a decrease in the cross sectional area, while $\pi_{t\ <110>}$ decreased with a increase in the aspect ratio of the cross section. The enhancement behavior of the $\pi_{l\ <110>}$ was explained qualitatively using 1-D hole transfer and hole conduction mass shift mechanisms. The reduction in the $\pi_{t\ <110>}$ with increase in the aspect ratio of the cross section is explained due to decreased stress transmission from the substrate to the

nanowire. The maximum value obtained of $\pi_{l\,<110>}$ of 48×10^{-11} Pa^{-1} at a surface concentration of 5×10^{19} cm^{-3}, indicate sufficient sensitivity for sensing applications.

Initial experimental studies undertaken by He and Yang [1] reported a very high piezoresistive effect (increased up to 3,776% with respect to the higher dimension counterparts) of self-assembled single crystal silicon nanowires in the <111> crystallographic orientation. Reck et al. [2] later used a lift-off and an electron beam lithography (EBL) technique to fabricate silicon test chips and studied the piezoresistive properties of crystalline and polycrystalline nanowires as a function of stress and temperature. They found that the piezoresistive effect in the <110> direction increased significantly as the silicon nanowire diameter decreased (up to 633%), consistent with the results from He and Yang [1]. Finally, Passi et al. [5] recently obtained an increase of piezoresistance of up to 2,140% respect to the bulk-Si in the same direction, the <110>.

To date, available published literature [1-5], [15], agree that low doping and surface-to-volume ratio represent the main parameters that boost the piezoresistance effect of SiNWs. Some hypotheses have been speculated on the origin of such phenomenon. Recently the major culprit has been indicated to be surface-state induced effect for nanowires smaller than 70nm width, and enhanced strain modulation of carrier mobility for larger nanowires [3].

Roylance and Angell introduced the first fully integrated piezoresistive micromachined accelerometers in 1978 for biomedical applications [15], [16]. An excellent literature review of micromachined piezoresistive accelerometers was provided by Barlian et al. [13] and interested readers are referred to their paper. Today, accelerometers are heavily commercialized MEMS application. They are widely used in automotive and space (crash detection, stability control and navigation [25]), biomedical (activity monitoring [27-29], surgical instrument tracking [24]), consumer electronics (portable computing, cameras lens stabilization, cellular phones), robotics (control and stability [26]), structural health monitoring, and military applications.

This paper presents the design and simulation of a single square millimeter 3-axial accelerometer for bio-mechanics detection [17], [18], [20]. The main requirements of this application are miniaturization and high measurement accuracy to allow the accelerometer to be implanted. In order to fulfil these requirements nanowires as nanoscale piezoresistive devices have been chosen as sensing element, due to their high sensitivity and potential in miniaturization.

2. Accelerometer Design

Initial technical specifications have been specifically designed in order to address the particular application requirements (impact measurement) [19], see table 1.

Table 1. Sensor technical specifications.

Range	*±250 G*
Sensitivity	4 mV/G
Frequency response	0 to 1,000 Hz
Shock limit	±1,000 G
Resolution	<10 mG
Non-Linearity	<1% FSO
Cross-Sensitivity	<5%
Dimension	<2×2×1 mm^3

The device range measurement is for medium-G impacts and the frequency response goes down to DC since bio-mechanics events, such as head injuries may have long duration transient.

The model of the sensing chip is shown in figure 1. The modeled geometry is an accelerometer with a highly symmetric micromechanical structure surrounded by four beams (figure 1) already available in the literature [23]. These types of geometries allow the minimizing of the overall cross-sensitivity due to a self-cancelling feature. The proof mass in red is suspended by four surrounding beams that resemble springs, while the damper is air in the model. Each beam is clamped-clamped to the fix frame and the

middle point is connected to the seismic mass. The overall geometric dimension of the chip is 1310 μm × 1310 μm × 400 μm. When acceleration is applied to the chip, the proof mass is displaced due to inertial force, resulting to beam deformation (figure 1) [23].
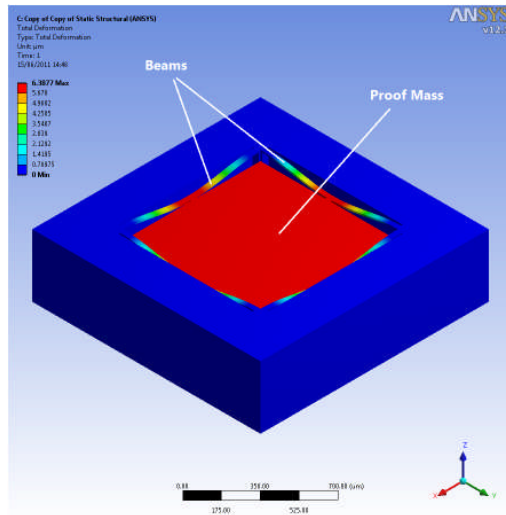

Figure 1. Model of the accelerometer under stress due to external forces. The red color corresponds to the maximum displacement of the proof mass. In blue is the surrounding frame which remains undeformed.

As it can be seen the beams change color gradually from blue to red due to deformation [23]. The beam deformation, due to the applied stress (σ) (figure 1), leads to a change in resistance (ΔR) of nanoscale piezoresistors proportional to the applied external inertial force (A). The fractional resistance change in the measurement circuit is proportional to the output voltage drop as well, therefore representing a measure of the acceleration.

2.1. Finite Element Structural Analysis
The material selected for the mechanical structure of the sensing element is anisotropic single crystal silicon (SCS), which has been chosen for its mechanical properties (good stress tensile strength and high gage factor) [22]. The modeled geometry has been analysed by about 350,000 meshing nodes and tetrahedron elements with the use of ANSYS 12.1 commercial software. First of all the inputs of the numerical model (geometry and material) have been validated against a readily available previous experimental work on a mechanical sensor demonstrator [23]. Table 2 presents the inputs parameters used in the developed FEM.

Table 2. Inputs geometric and material parameter used in the developed FEM.

Mechanical Structure material	Single Crystal Silicon Anisotropic
Density (kg/m^3)	2330
Young's Modulus [110] (GPa)	170
Poisson's Ratio [100]	0.28
Bulk Modulus (GPa)	128.8
Shear Modulus (GPa)	66.4
Longitudinal piezoresistive coefficient (Pa^{-1})	35×10^{-11} [23]
Length × width × thickness (mm)	2 × 2 × 0.45 [23]
Beams - Length × width × thickness (mm)	1 × 0.06 × 0.01 [23]

Because silicon is such an important economic material, these values have been investigated thoroughly, and the three independent stiffness coefficients of principal crystallographic orientations <100>, <010> and <001>, gives the following stiffness matrix [30], which has been used in the FEM developed:

$$[C] = \begin{bmatrix} 1.66 & 0.64 & 0.64 & 0 & 0 & 0 \\ 0.64 & 1.66 & 0.64 & 0 & 0 & 0 \\ 0.64 & 0.64 & 1.66 & 0 & 0 & 0 \\ 0 & 0 & 0 & 0.80 & 0 & 0 \\ 0 & 0 & 0 & 0 & 0.80 & 0 \\ 0 & 0 & 0 & 0 & 0 & 0.80 \end{bmatrix} \cdot 10^{11} Pa \tag{1}$$

The value of piezoresistive coefficient used for the sensitivity calculation is 35×10^{-11} Pa^{-1}, which is the value adopted by Dao et al. [23]. The simulation results of this study are on the same order of magnitude of the value of sensitivity obtained in the demonstrator device by Dao et al. [23]. Sensitivity under X-axis acceleration is 0.2 mV/g vs. 0.48 mV/g [23]; similar value is obtained under Y-axis acceleration. Under Z-axis acceleration the sensitivity is 0.314 mV/g vs. 0.56 mV/g [23]. Figure 2 compares the two studies.
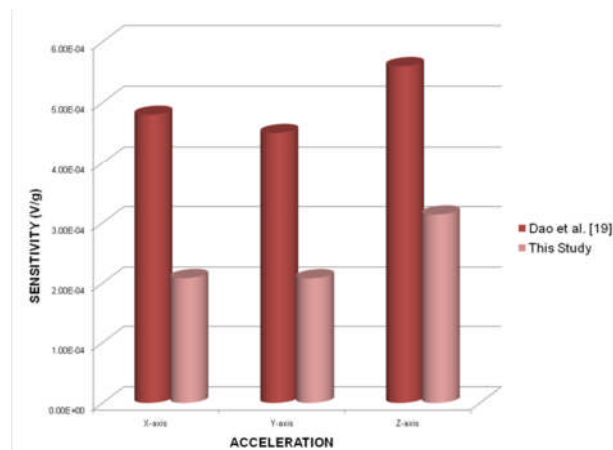

Figure 2. Validation of the model inputs by comparing to the demonstrator performance of Dao et al. [23].

After validation of our device against a real demonstrator we are able to further investigate on the design optimization of our model.

The optimization method uses an objective function which is to maximize the stress, using two constraints, the die size and the natural frequency. The results of the optimization process are as follows: 1st mode shape (ω_{oz}) of 5,277.7 Hz, the maximum equivalent stress (σ_{eq}) at 250G acceleration in the X or Y-axis are 44.837 MPa and 66.041 MPa in the microscale and nanoscale piezoresistors respectively. In the Z-axis σ_{eq} at 250G acceleration is 66.581 MPa and 99.243 MPa in the microscale and nanoscale piezoresistors respectively. By taking advantage of structure symmetry only the equivalent stress under X-axis acceleration as been analysed. The results for the Y-axis acceleration are equivalent.

Nanoscale piezoresistors, due to stress concentration region (i.e. the width is 10 times smaller than conventional piezoresistors), show an equivalent stress that is 47% higher than the conventional

counterparts under 250G. This increase represents an initial sensitivity enhancement for geometrical reasons. Clearly progressively reducing the dimension will upraise the stress concentration effect.

2.2. Nanoscale Piezoresistors Measurement Circuit

A total of 16 nanoscale piezoresistors were placed in strategic locations on the top surface of the mechanical structure (figure 3). Basically, in order to maximize the device electrical sensitivity, the piezoresistors were placed at the highest stress regions that were identified by FE stress distribution analysis.
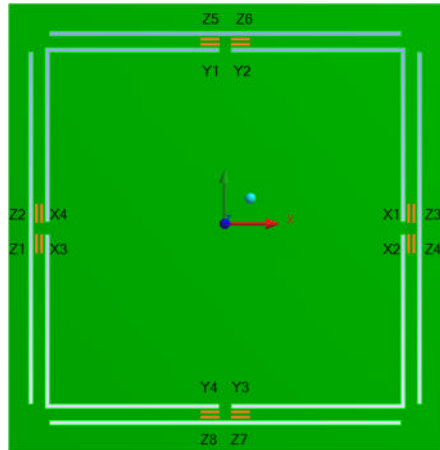

Figure 3. Piezoresistors location. 16 nanoscale piezoresistors, in orange, are placed in strategic location where is present the maximum stress in order to maximize the sensitivity and minimize the cross-sensitivity (top view).

The piezoresistors are interconnected in a measurement circuit by three full Wheatstone bridges, one for each axis-sensing, as in figure 4.
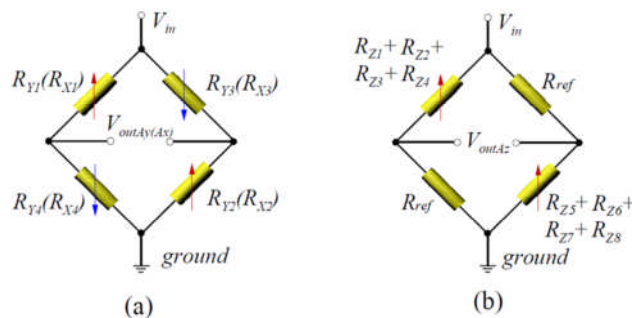
Figure 4. (a) A_x-, A_y-bridge and (b) A_z- Wheatstone Bridge measurement circuit

Hence, the change in resistance of piezoresistors is measured as output voltage drop by these bridges. The advantage of using a bridge is that as the four resistors are identical, the effect of the temperature coefficient can be cancelled out by the balanced configuration. Moreover, the highly symmetric geometry chosen for the structure allows a self-cancellation of part of the cross-axis acceleration since the piezoresistors are intentionally positioned symmetrically.

A detailed image of a nanoscale piezoresistor placed in one of the chip corner is presented in figure 5. Each piezoresistor is geometrically identical with a length of 3 micrometer and a width of 100 nanometers.

Figure 5. Nanoscale piezoresistor model.

3. Performance Calculation

3.1. Electrical sensitivity and cross-sensitivity
Table 3 summarizes the sensors performance calculation:

Table 3. Voltage noise, sensitivity, cross-sensitivity, resolution
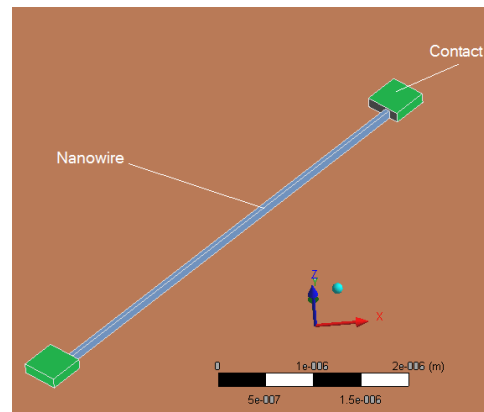
	Microscale		**Nanoscale**	
	Ax, Ay	**Az**	**Ax, Ay**	**Az**
V_{jn} **(μV)**	1.01	1.42	3.2	4.52
$V_{1/f}$ **(μV)**	0.4	0.28	13.14	9.29
V_{Noise} **(μV)**	1.2	1.97	13.53	10.41
Sensitivity (mV/g)	0.677	0.898	20.9	28.9
Cross-sensitivity (%)	-	-	0.061	0.0058
	-	-	2.779	0.0139
Resolution (mg)	1.78	2.2	0.64	0.36

The calculated electrical sensitivity of nanoscale piezoresistors in the <110> direction at low boron concentration at 37°C, increases of approximately 3,000% in comparison to the conventional ones, see table 3.

Cross-sensitivity is below 5% for all axes due to the highly symmetric geometry selected. The cross-axis sensitivities under the X-axis acceleration $S_{(Ax-Ay)\%}$ and $S_{(Ax-Az)\%}$ are detected respectively in the output of the A_y, A_z-bridge for the nanoscale piezoresistors.
These values are consequence of the highly symmetric geometry selected, the symmetric localizations of the piezoresistors on the top surface of the device and the measurement circuit (figure 3 and 8). Similar results are obtained for the microscale piezoresistors.

3.2. Noise
Noise is any output voltage that occurs when there is no acceleration applied to the sensor. There are three typical noise sources existing in all piezoresistive sensors, including the *Johnson noise* (noise floor or white noise), *Hooge's noise* (or 1/f noise, also called pink noise), and the *thermo-mechanical noise* (brown noise or Brownian noise).

The calculated Johnson noises corresponding to nanoscale and microscale piezoresistors are shown on the table 3. Johnson noise does not depend on the frequency. The noise in the nanoscale piezoresistors is increased by around 200% due to one order of magnitude greater resistance than conventional microscale ones. The total 1/f noise voltage corresponding to each measurement bridge is calculated to be

approximately 30 times greater in the nanoscale devices as clearly summarized on table 3. This is mainly due to the very low carrier concentration.

The thermo-mechanical noise corresponding to each component of acceleration at 37 °C with the calculated bandwidths at 5,539 Hz are in the order of few µg.

The total noise is calculated as the square root of the sum among the square power of each noise, as:

$$V_{Noise}^{Ax} = V_{Noise}^{Ay} = \sqrt{\left(V_{Jn}^{Ax}\right)^2 + \left(V_{1/f}^{Ax}\right)^2 + \left(V_{TM}^{x}\right)^2} \tag{2}$$

Similar equation has been applied for the Z-axis.

Noise analysis indicates that the total voltage noise in the accelerometer is increased by 10 times in the X and Y-axis, and 4 times in the Z-axis, see table 3.

The main contributor to the noise signal is the Hooge noise due to very low number of carriers in the nanoscale piezoresistors.

3.3. Resolution

The resolution of an accelerometer determines the minimum acceleration that can be measured. Resolution is defined as the noise divided by the sensitivity, therefore the resolution of the accelerometer is defined by (3) and (4) [23]:

$$R_{A_{x,y}} = \frac{V_{Noise}^{A_{x,y}}}{S_{Az}} \tag{3}$$

$$R_{A_{z}} = \frac{V_{Noise}^{A_{z}}}{S_{Az}} \tag{4}$$

Table 3 summarizes the sensor resolution calculated according to (26) and (27).

The resolution of the accelerometer with nanoscale piezoresistors is improved respect to the conventional microscale one of around 60-80% in all axes, due to their much higher sensitivity, see table 3. However, the noise level of the nanoscale piezoresistors is worse than the conventional microscale ones because Johnson and Hooge noises are dependent on the resistance value and numbers of carriers respectively. Therefore, given the doping concentration, smaller size means higher resistance and lower number of carriers.

4. Discussion

Table 4. Sensor comparison

	Microscale		Nanoscale	
	Present work	**Dao et al. [23]**	**Present work**	**Dao et al. [11]**
Range	Medium-G	Low-G	Medium-G	Low-G
Sensitivity (µV/g)	677	450	20,900	400
Resolution (mg)	1.78	0.9	0.64	14
Cross-Sensitivity (%)	2.78	5.5	2.78	-
Dimension (mm³)	1.3×1.3×0.4	2×2×0.45	1.3×1.3×0.4	0.5×0.5×0.35

The results obtained from the combined FE modeling, simulation of the mechanical structure and performance calculation of both MEMS and nanostructure are interesting for this field of study. Input

values used as piezoresistive coefficient for calculating the sensitivity and cross-sensitivity are obtained from experiments of Passi [5] for the nanostructure and Smith [21] for the microstructure. This study raises the attention on silicon nanowires structures as devices being embedded into mechanical sensors as piezoresistors. The improved resolution of the designed accelerometer (less than 1mg on all axes) compared to the conventional ones with 60-80% increase (see table 3) suggests that nanowires have the credential to be the sensing element of the future NEMS. This level of accuracy and precision of measurement is comparable to the capacitive counterparts' sensors.

To date only few laboratory prototypes have been fabricated, as reported by Dao et al. [11] suitable for low-G measurements. However, their device [11] sensitivity for each axis is only about 400 μVG^{-1}, and the resolution of 14 mg which requires further signal conditioning, see table 4.

This study instead presents a sensor with higher sensitivity obtained by calculations (20.9 mVG^{-1}), mainly because a higher stress on the nanowires. This is thanks to the optimization process undertaken that maximizes the stress on the beams of the mechanical structure, under the constraints specified (see table 1). The resolution and the sensitivity in this work is improved considerably compared to the work of Dao et al. [11] (see table 4) due to the fact that the sensor of Dao et al. is significantly smaller.

The designed sensor results suitable for the bio-mechanical application, such as head injuries monitoring. Finally, the total noise of nanoscale piezoresistors results are much higher than the conventional ones, however, since in the nanoscale structures the sensitivity grows faster than the noise level, the overall resolution is significantly improved. It is worthwhile to point out that our work is based on previous published experimental works on nanowires structures used as piezoresistors. Experimental studies are currently underway and will be reported in the next future.

5. Conclusion and Future work
This paper presents the design enhancement of a motion sensor for biomechanical measurement within a space-constrained environment. Due to the exploitation of electro-mechanical features of nanowires as nanoscale piezoresistors the nominal sensor sensitivity is overall boosted by more than 3,000%. This technology avoids the signal amplification but allows a higher resolution with the advantage of a smaller sensing element. Therefore, in comparison with conventional devices, the measured accuracy is considerably improved. Therefore, this study highlights the potential of silicon nanowires structure as piezoresistors embedded in future mechanical sensors.

6. Acknoledgement

References
[1]   He R and Yang P Giant piezoresistance effect in silicon nanowires 2006 *Nature Nanotechnol.* **1** issue 1 42–46
[2]   Reck K, Richter J, Hansen O and Thomsen E V Piezoresistive effect in top-down fabricated silicon nanowires 2008 *IEEE 21st Int. Conf. on Micro Electro Mechanical Systems* pp 717–720
[3]   Barwicz T, Klein L, Koester S J and Hamann H Silicon nanowire piezoresistance: Impact of surface crystallographic Orientation 2010 *Appl. Phys. Lett* vol 97 issue 2
[4]   Dao D V, Nakamura K, Bui T T and Sugiyama S Micro/nano-mechanical sensors and actuators based on SOI-MEMS technology 2010 *Adv. in Nat. Sciences: Nanoscience and Nanotechnology*
[5]   Passi V, Ravaux F, Dubois E, Raskin J-P Backgate bias and stress level impact on giant piezoresistance effect in thin silicon films and nanowires 2010 *IEEE MEMS 2010* pp 464 – 467
[6]   Lee M L, Fitzgerald E A, Bulsara M T, Currie M T and Lochtefeld A Strained Si, SiGe and Ge channels for high-mobility metal-oxide–semiconductor field-effect transistors 2005 *J. Appl. Phys.* **97** issue 1 011101-1
[7]   Haugerud B M, Bosworth L A and Belford R E Mechanically induced strain enhancement of metal-oxide–semiconductor field-effect transistors 2003 *J. Appl. Phys.* **94** issue 6 4102–4107

[8]   Chen L J Silicon nanowires: the key building block for future electronic devices 2007 *J. of Mat. Chem.* **17** issue 44 4639–4643

[9]   Toriyama T, Tanimoto Y and Sugiyama S Single crystal silicon nano-wire piezoresistors for mechanical sensors 2002 *J. Microelectromech. Syst.* **11** issue 5 605–611

[10] Toriyama T, Funai D and Sugiyama S Piezoresistance measurement on single crystal silicon nanowires 2003 *J. of Appl. Phys.* **93** issue 1 561–565

[11] Dao D V, Toriyama T and Sugiyama S. Noise and frequency analyses of a miniaturized 3-DOF accelerometer utilizing silicon nanowire piezoresistors 2004 *Proc. of IEEE, Sensors 2004* vol. 3 pp 1464–1467

[12] Shao M-W, Shan Y-Y, Wong N-B and Lee S-T Silicon Nanowire sensors for bioanalytical applications: Glucose and hydrogen peroxide detection 2005 *Adv. Funct. Mat.* **15** issue 9 pp 1478–1482

[13] Barlian A A, Park W-T, Mallon J R Jr, Rastegar A J and Pruitt B L Review: Semiconductor Piezoresistance for Microsystems 2009 *Proc. of the IEEE* vol 97 issue 3

[14] Okamura A, Dao D V, Toriyama T and Sugiyama S Fabrication of an ultra small accelerometer utilizing Si nanowire piezoresistors 2005 *Proc. of the 22nd Sensor Symposium* pp 203-206

[15] Roylance L M A miniature integrated circuit accelerometer for biomedical applications 1978 Ph.D. Electrical Engineering Department, Stanford University

[16] Roylance L M and Angell J A Batch-fabricated silicon accelerometer 1979 *IEEE Trans. Electron Devices* vol 26 issue 12 pp 1911–1917

[17] Stephen O E, Knox T and Cohn K A The development of a method to measure head acceleration and motion in high-impact crashes 2004 *Neurosurgery* vol 54 pp 672-677

[18] Nassiopoulos E and Njuguna J Finite element dynamic simulation of whole rallying car structure: towards better understanding of structural dynamics during side impacts 2011 *8th European LS-DYNA Conf.* p 31

[19] Wilson J S and Knovel 2005 *Sensor technology handbook* (Amsterdam; Boston: Elsevier)

[20] Unser M Motorsports accidentology 2009 MSc thesis School of Applied Sciences, Cranfield University, Cranfield, UK

[21] Smith C S Piezoresistance effect in germanium and silicon 1954 *Phys. Rev.* **94** issue 1 42-49

[22] Maluf N 2004 *An Introduction to Microelectromechanical Systems Engineering*, 2nd ed. (Boston: Arttech House)

[23] Dao D V, Okada S, Dau V T, Toriyama T and Sugiyama S 2004 Development of a 3-DOF Silicon Piezoresistive Micro Accelerometer *Proc. of the 2004 Int. Symp. on Micro-Nanomechatronics and Human Science and The Fourth Symp. Micro-Nanomechatronics for Information-Based Society*

[24] Ren H and Kazanzides P 2010 *IEEE/ASME Trans. On Mechatronics* vol **PP** issue 99

[25] Fang J, Zheng S, Han B 2011 Amb vibration control for structural resonance of double-gimbal control moment gyro with high-speed magnetically suspended rotor *IEEE/ASME Trans. On Mechatronics*, 10.1109/TMECH.2011.2161877

[26] Liljeback P, Pettersen K Y, Stavdahl O, Gravdahl J T 2011 Snake robot locomotion in environments with obstacles *IEEE/ASME Trans. On Mechatronics*, 10.1109/TMECH.2011.2159863

[27] Lawrence E, Navarro K F, Riudavets J, Messina M 2006 Macroscopic Sensor Networks: Application Issues in the Healthcare Industry *J. of Computational Methods in Sciences and Engineering* **6** issue 5, 6 supplement 2 309-319

[28] Messina M, Lawrence E, Navarro K F, Lubrin E 2007 Towards assistive healthcare: prototyping advances in wireless sensor network (WSN) system integration and application *IADIS International Conference - Wireless Applications and Computing (Lisbon)*

[29] Messina M, Lim Y Y, Lawrence E, Martin D, Kargl F 2008 Implementing and validating an environment and health monitoring system *5th Int. Conf. on Information Technology: New Generation ITNG (Las Vegas)*

[30] Kaajakari V 2009 Silicon as an anisotropic mechanical material *Practical MEMS: Analysis and design of microsystems, MEMS sensors, electronics, actuators, rf mems, optical mems, and microfluidic systems* (Small Gear Publishing) chapter 4 p 51